Mad1p, a Phosphoprotein Component of the Spindle Assembly Checkpoint in Budding Yeast

Kevin G. Hardwick and Andrew W. Murray

Department of Physiology, University of California, San Francisco, California 94143-0444

Abstract. The spindle assembly checkpoint prevents cells from initiating anaphase until the spindle has been fully assembled. We previously isolated mitotic arrest deficient (*mad*) mutants that inactivate this checkpoint and thus increase the sensitivity of cells to benomyl, a drug that interferes with mitotic spindle assembly by depolymerizing microtubules. We have cloned the *MAD1* gene and show that when it is disrupted yeast cells have the same phenotype as the previously isolated *mad1* mutants: they fail to delay the metaphase to anaphase transition in response to microtubule depolymerization.

MAD1 is predicted to encode a 90-kD coiled–coil protein. Anti-Mad1p antibodies give a novel punctate nuclear staining pattern and cell fractionation reveals that the bulk of Mad1p is soluble. Mad1p becomes hyperphosphorylated when wild-type cells are arrested in mitosis by benomyl treatment, or by placing a cold sensitive tubulin mutant at the restrictive temperature. This modification does not occur in G1-arrested cells treated with benomyl or in cells arrested in mitosis by defects in the mitotic cyclin proteolysis machinery, suggesting that Mad1p hyperphosphorylation is a step in the activation of the spindle assembly checkpoint. Analysis of Mad1p phosphorylation in other spindle assembly checkpoint mutants reveals that this response to microtubule-disrupting agents is defective in some (*mad2*, *bub1*, and *bub3*) but not all (*mad3*, *bub2*) mutant strains. We discuss the possible functions of Mad1p at this cell cycle checkpoint.

ACCURATE chromosome replication and segregation require mechanisms that can detect errors in these processes and initiate two responses: repair systems that correct the errors, and delay mechanisms that prevent the cell cycle from proceeding while the repairs are in progress. The combined detection and delay systems are known as cell cycle checkpoints or feedback controls (reviewed in Hartwell and Weinert, 1989; Murray, 1994, 1995).

Genetic analyses in both budding and fission yeast have identified a number of genes that play a role in ensuring that cells complete DNA replication and repair DNA damage before they enter mitosis (Weinert and Hartwell, 1988; Enoch and Nurse, 1990; Al-Khodairy and Carr, 1992; Rowley et al., 1992; Enoch et al., 1992; Weinert et al., 1994; Al-Khodairy et al., 1994, 1995; Ford et al., 1994). For example, the *RAD9* gene is required to arrest the cell cycle in response to DNA damage, but is not required for the process of DNA repair (Weinert and Hartwell, 1988). This cell cycle control is not essential for growth in the absence of DNA damage, but irradiated *rad9* cells are unable to delay their passage through mitosis in response to the damaged DNA and produce lethally damaged progeny.

The mitotic arrest caused by microtubule polymerization inhibitors suggests the existence of a spindle assembly checkpoint that monitors the status of the spindle and regulates the metaphase to anaphase transition. The ability of single improperly oriented chromosomes (Callan and Jacobs, 1957; Li and Nicklas, 1995; Rieder et al., 1994), partially defective centromeres (Spencer and Hieter, 1992), and excess centromeres (Futcher and Carbon, 1986; Wells, W., and A. W. Murray, unpublished results) to delay anaphase suggests that this checkpoint can detect subtle as well as gross defects in the structure of the spindle. Mutants in the spindle assembly checkpoint have been identified in budding yeast. The *bub* (budding uninhibited by benzimidazole; Hoyt et al., 1991) and *mad* (mitotic arrest deficient; Li and Murray, 1991) mutants were isolated from collections of mutants that failed to form colonies in the presence of low doses of benomyl, a microtubule polymerization inhibitor. The *mad* mutants were distinguished from mutants that affected microtubule assembly by their inability to delay cell division in response to microtubule depolymerization. The divisions that take place in the absence of a fully functional spindle lead to a high frequency of chromosome loss and cell death (Li and Murray, 1991). The spindle assembly checkpoint defined by the *mad* and

Address all correspondence to A. W. Murray, Department of Physiology, Box 0444, University of California, 513 Parnassus Avenue, San Francisco CA 94143-0444. Ph.: (415) 476-0364. Fax: (415) 476-4929.

Table I.

		Yeast strains
KH 34	a	*ura3-1, leu2,3-112, his3-11, trp1-1, ade2-1, can1-100*
KH 35	α	*ura3-1, leu2,3-112, his3-11, trp1-1, ade2-1, can1-100*
KH 36	a/α	*ura3-1/ura3-1, leu2,3-112/leu2,3-112, his3-11/his3-11, trp1-1/trp1-1, ade2-1/ade2-1, can1-100/can1-100*
KH 120	a	*mad1-1, his3, leu2, ura3-52*
BEN 24	a	*mad1-1, his3, leu2, ura3-52, rad9Δ::LEU2*
BEN 27	a	*mad1-2, his3, leu2, ura3-52, rad9Δ::LEU2*
BEN 79	a	*mad1-3, his3, leu2, ura3-52, rad9Δ::LEU2*
KH 123	a	*mad1Δ.1::HIS3, ura3-1, leu2,3-12, his3-11, trp1-1, ade2-1, can1-100*
KH 131	a	*mad1Δ.2::URA3, ura3-1, leu2,3-112, his3-11, trp1-1, ade2-1, can1-100*
KH 132	a	*mad2-1, ura3-1, leu2,3-112, his3-11, trp1-1, ade2-1, can1-100*
KH 125	a	*mad3Δ::LEU2, ura3-1, leu2,3-112, his3-11, trp1-1, ade2-1, can1-100*
KH 40	a	*cin1Δ::HIS3, ura3-1, leu2,3-112, his3-11, trp1-1, ade2-1, can1-100*
KH 127	a	*bub1Δ::HIS3, ura3-1, leu2,3-112, his3-11, trp1-1, ade2-1, can1-100*
KH 128	a	*bub2Δ::URA3, ura3-1, leu2,3-112, his3-11, trp1-1, ade2-1, can1-100*
MAY 2072	a	*bub3Δ::LEU2, ura3-52, leu2,3-112, his3-Δ200, lys2-801*
KH 161	a	*cdc15-2, ura3-1, leu2,3-112, his3-11, trp1-1*
KH 162	a	*cdc23, ura3-1, leu2,3-112, trp1-1, ade2-1*
KH 152	a	*tub2-403, ura3-52, leu2,3-112, lys2-801*
KH 146	a	*ura3-52, leu2,3-112, trp1-1*

bub mutants is expected to consist of components that detect defects in spindle structure, and a signal transduction pathway that relays this information and ultimately inhibits a target in the machinery that initiates sister chromatid separation and anaphase. In common with other cell cycle transitions a major regulator of the metaphase to anaphase transition is thought to be the kinase activity of Cdc28p-mitotic cyclin complexes (for reviews see Norbury and Nurse, 1992; Morgan, 1995). Experiments in frog egg extracts and in yeast have shown that the ubiquitin-mediated proteolysis of mitotic cyclins and other proteins is required for sister chromatid separation and entry into the next cell cycle (Holloway et al., 1993; Surana et al., 1993).

Little is known about the biochemical mechanism of the spindle assembly checkpoint. Previous work has shown that *BUB1* encodes a protein kinase (Roberts et al., 1994) and that *BUB2*, *BUB3* (Hoyt et al., 1991), and *MAD2* (Chen, R-H., and A. W. Murray, unpublished results) encode proteins with unknown biochemical functions. Here we report the cloning of the *MAD1* gene and show that it encodes a novel nuclear phosphoprotein that is an essential component of the spindle assembly checkpoint, but is not essential for growth under normal conditions. We find that this protein is hyper-phosphorylated in conditions that activate the spindle assembly checkpoint. The hyper-phosphorylation of Mad1p is only seen in a subset of *mad* and *bub* mutants allowing us to provisionally order the function of the known *BUB* and *MAD* genes.

Materials and Methods

Yeast Strains and Media

Table 1 lists the strains used in this work. The original *mad1* mutants were isolated in the A364A background. All other strains are derivatives of W303, except the *bub3Δ* strain MAY 2072 (Hoyt et al., 1991) and the *tub2-403* (KH 152) and corresponding *TUB2* control (KH146) strain which are S288C derived. Media were prepared and genetic manipulations were performed as described (Sherman et al., 1974). Stock solutions of inhibitors were: benomyl 30 mg/ml in DMSO (added to hot media to maintain solubility), hydroxyurea 200 mg/ml in water, and α-factor 10 mg/ml in DMSO. Microcolony assays were carried out as previously described (Li and Murray, 1991).

Cloning of MAD1

Earlier attempts to clone the *MAD1* gene using centromeric and multicopy libraries were unsuccessful, although we isolated a number of multicopy suppressors that conferred benomyl resistance on a variety of *mad* mutants and a mutant (*cin1Δ*) with defects in microtubule polymerization (Stearns et al., 1990). These suppressors included the transcription factors *YAP1* (also named *PAR1*, *SNQ3*, and *PDR4*) and *CAD1* along with a novel member of the hsp70 family, whose sequence will be reported elsewhere. The two transcription factors had been previously isolated in multi-copy suppressor screens due to their ability to confer multi-drug resistance on yeast cells (Moye-Rowley et al., 1989; Hussain and Lenard, 1991; Schnell et al., 1992; Wu et al., 1993).

Assuming that the *MAD1* gene was not present, or was at best poorly represented, in the available libraries, we constructed a new YCP50-based genomic library. We prepared genomic DNA as previously described (Philippsen et al., 1991) from W303 strain KH 34, carried out a partial *Sau3A* digest, isolated 6–10-kb fragments, and ligated them to BamHI cut and phosphatase-treated YCP50 (Rose et al., 1987). This ligation was transformed into *Escherichia coli* strain XL1-Blue MRF (Stratagene, La Jolla, CA) and four pools of ~10,000 colonies each were used to isolate plasmid DNA. This library DNA was then used to transform the *mad1-1* strain KH 120. After two to three days of growth on uracil-free plates the Ura^+ yeast transformants were scraped off, diluted, and replated onto YPD plates containing 10 μg/ml benomyl. Plasmid DNA was prepared (Ward and Kirschner, 1990) from benomyl-resistant colonies and individual plasmid isolates were re-tested for their ability to confer benomyl resistance to KH 120. One plasmid, pKH130, with a 6.2-kb insert, had this property. A 3.2-kb HindIII-SalI fragment from this plasmid was sufficient to complement *mad1* strains. This fragment contained unique XhoI and XbaI sites. When either the XhoI or the XbaI restriction site was filled in, the resulting clone no longer complemented the *mad1* mutant, suggesting that these sites lay within, or near, the complementing gene.

To check that the HindIII-SalI fragment contained the *MAD1* gene rather than a suppressor we cloned the flanking HindIII fragment into the *URA3*-containing integration vector pRS306 (Sikorski and Hieter, 1989). This construct was cut with BglII then transformed into the *mad1, ura3* strain, KH 120, to create a *mad1* strain in which the genomic locus of the cloned gene was marked with *URA3*. This strain was then mated with KH 35, a *MAD1, ura3* strain, the resulting diploids were sporulated and tetrads were dissected. In 10 tetrads the *mad* phenotype co-segregated with the Ura^+ spores, confirming that the sequences in pKH130 are closely linked to *MAD1*.

Sequencing, Mapping, and mad1 Gene Disruptions

We sequenced the whole of the 3,188-bp HindIII-SalI fragment, after subcloning various fragments into pBluescript and making ExoIII deletion series (Henikoff, 1984). We found a single large open reading frame that is predicted to encode a protein of 749 amino acids. The sequence of this reading frame was completed and confirmed on the second strand using specifically designed primers.

The *MAD1* reading frame was used to make a digoxygenin-labeled probe with a DNA labeling kit (Boehringer-Mannheim Corp., Indianapolis, IN) following the manufacturers instructions. This was used to probe a set of filters purchased from the American Type Culture Collection (Rockville, MD) that have DNA from lambda and cosmid clones covering over 96% of the genome of *Saccharomyces cerevisiae* cross-linked to them. The *MAD1* probe specifically recognized a single lambda clone (70269) thereby mapping it to the left arm of chromosome VII between *RAD6* and *CYH2*.

Two *mad1* gene disruptions were made (see Fig. 1): one, *mad1Δ1*, replaces the HincII fragments from nucleotides 994 to 2,186 with a BamHI fragment containing the *HIS3* gene (pKH149). The other, *mad1Δ2*, replaces almost the complete *MAD1* reading frame from the BglII site at position 76 to the XmnI site at 1911 with the *URA3* marker (pKH160). These constructs were used to transform haploid and diploid strains (KH 34, 35, and 36). Benomyl-sensitive haploid transformants were recovered and the gene disruptions confirmed using both PCR and Western blotting analyses (see Fig. 4).

Preparation of Antibodies against Mad1p, Immunoblotting, and Immunofluorescence

The BglII fragment encoding residues 27 to 310 of Mad1p was cloned into the BamHI site of pGEX3X (Smith and Johnson, 1988). This glutathione-*S*-transferase (GST)[1] fusion construct was transformed into *E. coli* strain HB101 and its expression induced with 0.1 mM IPTG for 3 h at room temperature. Cells were pelleted and resuspended on ice with PBS (140 mM Na_2HPO_4, 1.8 mM KH_2PO_4, 138 mM NaCl, 2.7 mM KCl, pH 7.2), repelleted, and frozen in liquid nitrogen. The frozen cells were resuspended in five volumes of PBS containing 1 mM EDTA, 1 mM EGTA, 1 mM $MgCl_2$, 1 mM PMSF, 200 μg/ml lysozyme, and 5 μg/ml DNase. To complete their lysis the cells were sonicated briefly. KCl was added to 0.25 M and DTT to 15 mM and the lysate was spun at 35,000 rpm in a rotor (model 50.2 Ti; Beckman Instruments, Palo Alto, CA) for 1 h. The supernatant was then loaded onto a 10 ml glutathione agarose column (Sigma Chemical Co., St. Louis, MO) which was then washed with PBS containing 0.25 M KCl and 0.5 mM DTT. The Mad1-GST fusion protein was eluted with 5 mM reduced glutathione in 50 mM Tris, pH 8.1, 0.25 M KCl. The peak fractions were dialyzed extensively into 50 mM Hepes, pH 7.6, 50 mM KCl, 30% glycerol. This protein was sent to Berkeley Antibody Company (Berkeley, CA) where it was used to immunize a rabbit. The rabbit serum was passed over a 50 ml column of GST fusion protein coupled to Affigel 10 (Bio-Rad Labs, Hercules, CA) to remove anti-GST antibodies, then affinity purified using a 5 ml column of the Mad1p–GST fusion protein coupled to Affigel 10.

Yeast extracts for immunoblotting were made by bead-beating cells in SDS sample buffer (80 mM Tris, pH 6.8, 2% SDS, 10% glycerol, 10 mM EDTA, 0.0013% Bromphenol blue, 50 mM NaF, 100 μM NaVanadate, 1 mM PMSF and LPC [10 μg/ml leupeptin, pepstatin, and chymostatin]). Standard methods were used for SDS-PAGE and protein transfer to nitrocellulose (Harlow and Lane, 1988). Blots were stained with Ponceau S to confirm transfer and equal protein loading, then blocked for 30 min with blotto (4% dried milk, PBS, 0.1% Tween 20). The affinity-purified anti–Mad1p antibody (0.5 mg/ml glycerol stock) was used at a dilution of 1:5,000 in blotto, and the anti-Clb2p antibody (1 mg/ml glycerol stock; kindly provided by Doug Kellogg, University of California, Santa Cruz, CA) at 1:1,500, either overnight at 4°C or for 2 h at room temperature. After washing extensively in PBS the blots were then incubated with HRP-conjugated anti–rabbit antibodies (Amersham Corp., Buckinghamshire, UK) at a 1:5,000 dilution, washed again, and developed using Amersham ECL detection reagents following the manufacturer's instructions.

The affinity-purified anti–Mad1p antiserum still recognizes a number of other proteins in addition to Mad1p on immunoblots of whole yeast cell extracts including a prominent band at 85 kD (see Fig. 4). However, these cross-reacting proteins are not immunoprecipitated by the antibody (see Fig. 9), nor are they recognized well in formaldehyde-fixed yeast cells (see Fig. 5), suggesting that they are unlikely to be closely related to Mad1p. Attempts have been made to reduce the background on the immunoblots, by using higher salt concentrations and other blocking agents such as BSA, but the conditions used here provide the optimal detection of Mad1p and its hyperphosphorylated forms.

For solubility studies, spheroplasts were prepared by treating logarithmically growing cells (KH 34) with 100 mM Tris, pH 9.4, 10 mM DTT for 10 min at room temperature, and then digesting the cell walls with lyticase in YPD containing 0.7 M sorbitol and 10 mM Tris, pH 7.4, for 15 min at 30°C. Spheroplasts were washed and allowed to recover for 30 min at room temperature in YPD containing 0.7 M sorbitol, washed in ice-cold lysis buffer (0.2 M sorbitol, 20 mM Hepes, pH 6.8, 50 mM KOAc, 2 mM EDTA, 0.5 mM EGTA, LPC, 1 mM PMSF), and then dounced 20 times. This homogenate was spun at 7,000 *g* in a Beckman TL100.3 rotor and the pellet resuspended in lysis buffer and dounced and spun once again to remove any remaining whole cells and debris. DTT was added to 1 mM to the pooled supernatants, and aliquots were treated with the following: 1% Triton X-100, 1 M NaCl or 1% Triton X-100 with 1 M NaCl and 0.25 mg/ml DNase/RNase. After 60 min the extracts were spun at 50,000 rpm in a Beckman TL100.2 rotor for 30 min. The supernatant fractions were precipitated with TCA and equivalent fractions of pellet and supernatant fractions separated by SDS-PAGE.

For gel filtration, yeast extracts were made by bead-beating whole cells (KH 34) in 50 mM Hepes, pH 7.6, 25 mM KCl, 50 mM NaF, 1 mM $MgCl_2$, 1 mM EGTA, 0.1% NaDeoxycholate, 10% glycerol, LPC, 1 mM PMSF, 0.5 mM DTT. The lysate was spun briefly to remove the glass beads and cell debris and then spun for 30 min at 55,000 rpm in a Beckman TL100.2 rotor. 200 μl was loaded on to a Superose 6 HR 10/30 column (Pharmacia Biotech Inc., Piscataway, NJ) running at 0.3 ml/min and 0.5 ml fractions were collected. For sucrose-gradient centrifugation a bead-beaten extract was made in 50 mM Hepes, pH 7.6, 50 mM KCl, 50 mM NaF, 1 mM $MgCl_2$, 1 mM EGTA, 0.1% NaDeoxycholate, LPC, 1 mM PMSF, 0.5 mM DTT, and spun for 30 min at 55,000 rpm in a TL100.2 rotor. A 2 ml sucrose gradient (5–40%) was made using a SG5 gradient mixer (Hoefer Scientific Instruments, San Francisco, CA), 100 μl of extract was loaded on top, and spun in a TLS55 swinging-bucket rotor at 55,000 rpm for 14 h. 75 μl fractions were taken from the top of the gradient. The sucrose gradient and the gel filtration column were calibrated with markers from a Pharmacia high molecular weight calibration kit.

For immunofluorescence, spheroplasts were prepared as above then fixed with 3.7% formaldehyde for 5 to 30 min, gently sedimented, washed, and resuspended in 0.7 M sorbitol, 0.1 M KPO_4, pH 7.5, before being attached to poly-lysine–coated multi-well microscope slides. The slides were plunged into methanol (−20°C) for 5 min and acetone (−20°C) for 30 s, and then allowed to air dry. After washing with PBS, cells were blocked for 30 min with blotto, and then stained overnight at 4°C with primary antibody diluted (1:5,000 for anti-Mad1p, 1:200 for anti-tubulin, 1:1,000 for anti-Rap1p, 1:2,000 for mAb 414) in blotto. Cells were washed several times with blotto and then incubated for 1 h at room temperature with a 1:50 dilution of FITC or rhodamine-labeled anti–rabbit, mouse or rat secondary antibodies from Cappel (Organon Teknika Corp., Durham, NC). After washing with blotto and then PBS, the DNA was stained with 1 μg/ml DAPI in PBS and cells were mounted in 90% glycerol, 1 mg/ml phenylenediamine, pH 9.0. Coverslips were sealed with clear nail polish and slides stored at −20°C.

Phosphate Labeling and Phosphatase Digestion

Cells were grown overnight in low-phosphate YPD medium (Rubin, 1975), diluted into fresh medium and grown to log phase. 1 mCi [^{32}P]orthophosphate (Amersham Corp.) was added to 5 ml cultures which were shaken at room temperature for one hour. Cells were pelleted, washed, and resuspended on ice in RIPA buffer (50 mM Hepes, pH 7.6, 150 mM NaCl, 1% Triton-X 100, 1% NaDeoxycholate, 0.1% SDS, 1 mM PMSF, LPC, 1 mM DTT, 50 mM NaF, 1 mM NaVanadate). An equal volume of glass beads was added and the cells were bead-beaten for 2 min at 4°C. Extracts were clarified, diluted to 1 ml with RIPA buffer and then 1 μl of anti-Mad1p antibody and 10 μl of protein A–Sepharose 6MB (Pharmacia) beads were added and incubated overnight at 4°C. Immunoprecipitates were washed several times with RIPA buffer, twice with PBS and once again with RIPA before heating the beads in sample buffer and separating the sample by SDS-PAGE. Gels were stained, fixed, dried down, and exposed to film overnight at −80°C.

1. *Abbreviations used in this paper*: GST, glutathione-*S*-transferase; LPP, lambda protein phosphatase.

For lambda protein phosphatase (LPP) treatments whole cell extracts were made by bead-beating yeast cells for 2 min in lysis buffer (50 mM Hepes, pH 7.6, 75 mM KCl, 1 mM $MgCl_2$, 1 mM EGTA, 0.1% NP40, 1 mM PMSF, LPC, 50 mM NaF, 1 mM NaVanadate) and DTT was added to 1 mM after clarification. Mad1p was immunoprecipitated as described above and the immunoprecipitate was washed three times with lysis buffer, twice with PBS and then with LPP reaction buffer (50 mM Tris, pH 8.0, 2 mM $MnCl_2$, 1 mM PMSF, LPC, 1 mg/ml acetylated BSA). 20 U of lambda protein phosphatase (New England Biolabs Inc., Beverly, MA) were added to the Mad1p immunoprecipitate in 50 μl of LPP reaction buffer and incubated for 30 min at 30°C. Phosphatase inhibitors were 2 mM $ZnCl_2$, 1 mM NaVanadate and 50 mM NaF. The Sepharose beads were then spun down and heated in sample buffer before separating the sample by SDS-PAGE and analyzing Mad1p by immunoblotting.

Results

MAD1 Is Predicted to Encode a Novel Coiled–Coil Protein

We cloned the wild-type *MAD1* gene by complementing the benomyl sensitivity of the *mad1-1* mutant. The complementing plasmid rescued all three *mad1* alleles, did not rescue other benomyl sensitive mutants, and contained a DNA fragment that is closely linked to the *MAD1* gene (see Materials and Methods). Sequencing the minimal complementing DNA fragment revealed a 2,250-bp reading frame which spans both an XhoI site and an XbaI site. Filling in either the XhoI site or the XbaI site destroyed the ability of this fragment to complement *mad1*. Two gene disruptions were made, one replacing the 3′ half of the *MAD1* gene with *HIS3* and a second that replaced almost the whole reading frame with the *URA3* gene (see Fig. 1 and Materials and Methods). These constructs were used to transform haploid and diploid yeast strains. The disrupted haploid strains grow as well as wild-type cells at all temperatures tested, are sensitive to anti-microtubule drugs (see Fig. 3 *a*), and are unable to complement the *mad1* alleles previously isolated confirming that the disrupted reading frame is indeed *MAD1*.

The DNA sequence and predicted translation of *MAD1* is shown in Fig. 2 *a*. The amino acid sequence of Mad1p shows about 20% identity to a large number of proteins that contain or are predicted to contain regions of coiled–coil (e.g., myosin, integrins, NuMA [Yang et al., 1992], CENP-E [Yen et al., 1992], Uso1p [Nakajima et al., 1991]). This homology is mainly due to the presence of heptad repeats of hydrophobic residues, which are found throughout the *MAD1* reading frame. Using the GCG computer program PEPCOIL we found that the bulk of Mad1p does

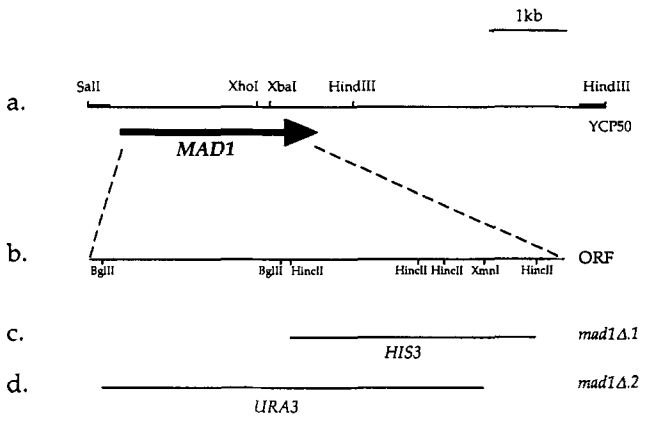

Figure 1. Restriction map of the *MAD1* clone and gene disruptions. (*a*) Restriction map of the *MAD1* clone isolated from the YCP50 library showing the position of the open reading frame (*ORF*). Vector sequences are indicated by the thicker line. (*b*) Restriction map of the open reading frame (*ORF*). (*c*) The bar marks the HincII fragments that were replaced with the *HIS3* gene to create *mad1Δ.1*. (*d*) The bar marks the BglII-XmnI fragment that was replaced with the *URA3* gene to create *mad1Δ.2*.

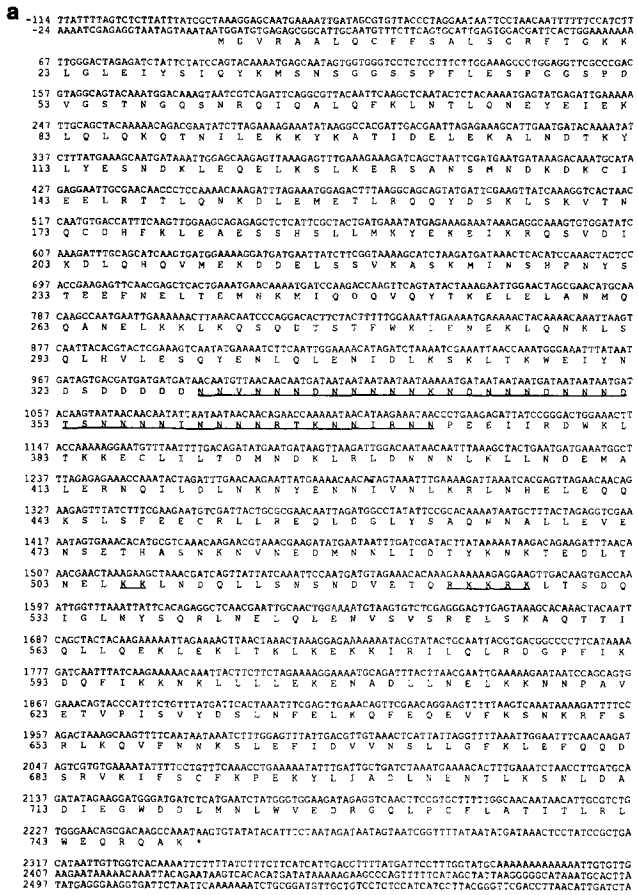

Figure 2. (*a*) Nucleotide sequence and translation of the *MAD1* gene. An unusual stretch of asparagine residues and the putative bi-partite nuclear localization signal are underlined. This sequence is available from Genbank/EMBL/DDBJ under accession number U14632. (*b*) Coiled–coil prediction for Mad1p. This GCG PEPCOIL prediction uses the algorithm of Lupas et al. (1991) with a window of 28 residues.

indeed have a high probability of forming coiled–coil (see Fig. 2 *b*) (Lupas et al., 1991). The sequence of Mad1p also contains a putative bi-partite nuclear localization sequence (residues 506–527) (Dingwall and Laskey, 1991), many potential phosphorylation sites and an unusual stretch rich in asparagine residues (residues 330–372).

The MAD1 Gene Encodes a Component of the Spindle Assembly Checkpoint

We studied *mad1Δ* strains for defects in the spindle assembly checkpoint. The benomyl sensitivity of the original *mad* mutants could be rescued with hydroxyurea, a drug that lengthens S phase (Li and Murray, 1991). Since budding yeast can assemble a spindle during S phase, our interpretation of this result is that the enforced delay in S phase allows *mad* cells enough time to correctly assemble their mitotic spindle before initiating anaphase. Although 1 mg/ml hydroxyurea slightly decreases the benomyl sensitivity of wild-type cells, it does not rescue the benomyl sensitivity of mutants with defects in microtubule polymerization, such as *cin1Δ* (Fig. 3 *a*), even at lower concentrations of benomyl (data not shown). Fig. 3 *a* shows that the *mad1Δ.1* deletion mutant behaves like the original *mad1* and *mad2-1* alleles: at 23°C it is sensitive to benomyl at concentrations of 7.5 μg/ml and above, and this benomyl sensitivity can be rescued by 1 mg/ml hydroxyurea.

We used microcolony assays to monitor the initial rate of cell division of *mad1Δ.1* strains on benomyl-containing medium. Individual, unbudded cells were picked with a dissecting needle and their growth on plates containing 12 μg/ml benomyl was analyzed over a period of 8 hours. Fig. 3 *b* shows that, like the original *mad1* alleles, the *mad1Δ.1* strain initially divided faster than the wild-type control cells. This behavior of *mad1Δ.1* differs radically from strains with defects in microtubule polymerization, which are unable to divide in the presence of benomyl and arrest as large budded cells. This result is consistent with *mad1Δ.1* cells being unable to sense or respond to the disruption of their microtubules and thus initiating anaphase before spindle assembly is complete. It has previously been shown that *mad* mutants fail to maintain the mitotic activity of Cdc28p (monitored as histone H1 kinase activity) when they are treated with benomyl (Li and Murray, 1991). We have confirmed this result with *mad1Δ.1* (data not shown).

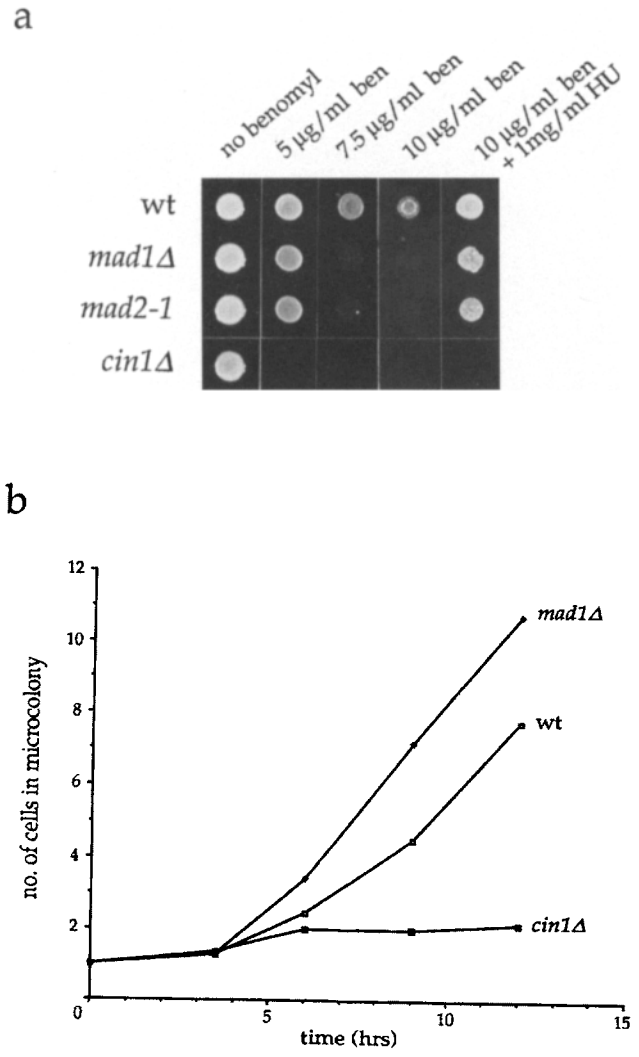

Figure 3. Benomyl sensitivity of the *mad1Δ.1* strain (KH 123). (*a*) Yeast cells (KH 34, KH 123, KH 132, and KH 40) were spotted onto YPD plates containing the indicated concentrations of benomyl and hydroxyurea and were photographed after 3 d of growth at 23°C. (*b*) Microcolony analysis of the growth of yeast cells (KH 34, KH 123, and KH 40) on YPD plates containing 12 μg/ml benomyl at 23°C. Data was collected from at least 60 cells of each genotype.

Mad1p Is a Soluble Nuclear Protein

To analyze the properties of Mad1p we raised polyclonal antibodies, against a GST fusion protein that contained

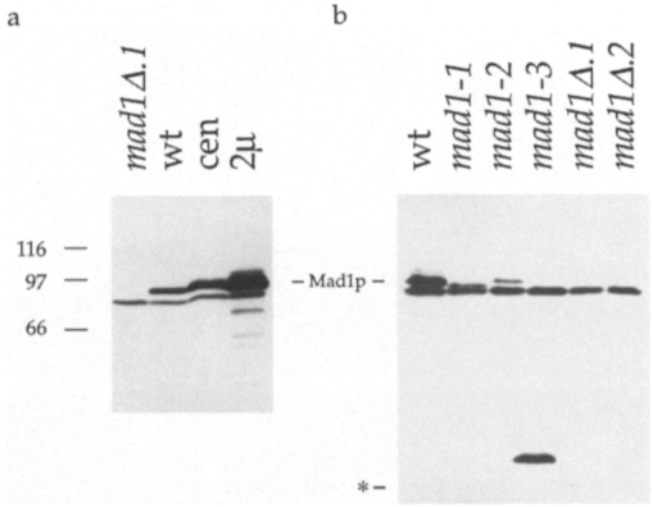

Figure 4. Immunoblots of yeast extracts with anti-Mad1p. (*a*) Whole cell extracts made from *mad1Δ.1* cells (KH 123), wild-type cells (KH 34) or wild-type cells containing the *MAD1* gene on a centromeric (pKH130) or two-micron (pKH137) plasmid were immunoblotted with affinity-purified anti–Mad1p antibodies. (*b*) Whole cell extracts made from wild-type (KH 34), the three original *mad1* alleles (BEN 24, 27, and 76), or the two *mad1* deletion strains constructed (KH 123, KH 131), were immunoblotted with affinity-purified anti–Mad1p antibodies. The truncated protein expressed in *mad1Δ.1* is indicated (*).

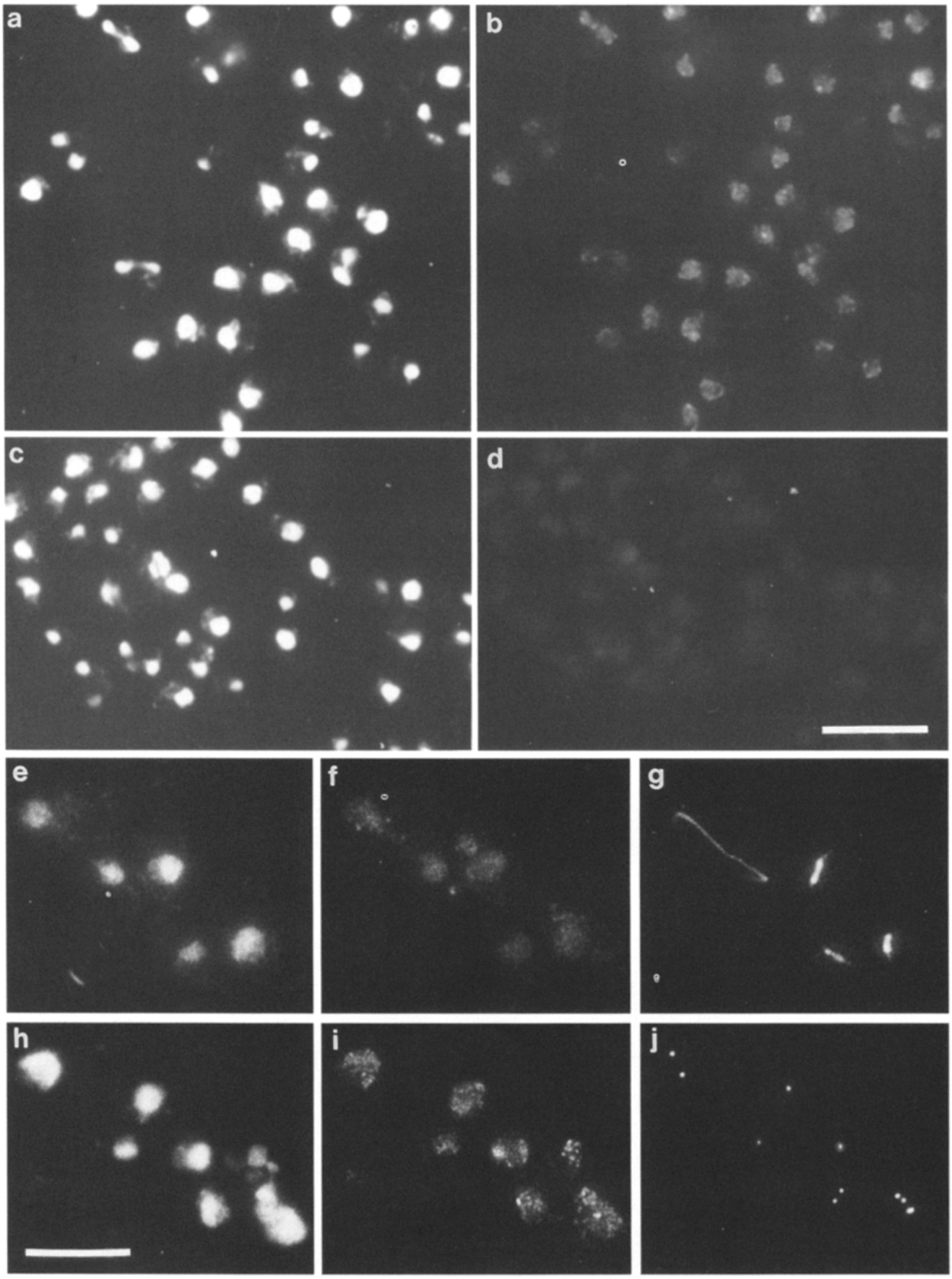
a
b
c
d
e
f
g
h
i
j

the amino-terminal half of Mad1p. The serum was affinity purified and used to probe Western blots of whole cell extracts from a number of yeast strains. Fig. 4 *a* shows that a protein of 90 kD that is seen in the wild-type cell extract is absent from the *mad1Δ.1* strain, and present at higher levels in strains containing *MAD1* plasmids. A truncated Mad1 protein is expressed in *mad1Δ.1* where the 3′ end of the *MAD1* gene has been removed, and in two of the three previously isolated *mad1* alleles (Fig. 4 *b*). The latter finding provides strong evidence that the reading frame we have identified is indeed the *MAD1* gene and that the antiserum efficiently recognizes both wild-type and a number of mutant Mad1 proteins. The affinity-purified anti–Mad1p antiserum still recognizes a number of other proteins in addition to Mad1p on immunoblots of whole yeast cell extracts, including a prominent band at 85 kD. However, the cross-reacting proteins are not immunoprecipitated by the antibody (see Fig. 9), nor are they recognized well in formaldehyde-fixed yeast cells (Fig. 5), suggesting that they are unlikely to be closely related to Mad1p.

Immunofluorescence with affinity-purified anti–Mad1p antibodies was used to localize Mad1p within yeast cells. Fig. 5 reveals that the bulk of Mad1p appears as discrete patches in the nucleus. The reactivity of Mad1p is sensitive to fixation. We found that greater than 5 min of formaldehyde fixation dramatically reduced Mad1p staining and further fixation completely abolished it (data not shown). We used a number of antibodies to confirm that the structure of the yeast nucleus was relatively intact after fixation. Fig. 5 (*e–j*) shows that antibodies to tubulin (Adams and Pringle, 1984) and to the 90-kD component of the spindle–pole body (Rout and Kilmartin, 1990) gave the previously reported patterns, and that there was no consistent co-localization of these proteins with Mad1p. In addition, we found no co-localization of Mad1p with Rap1p (a telomere protein; Klein et al., 1992) or nuclear pore antigens (data not shown). Although we observed coincident localization of some of the Mad1p staining and spindle pole bodies in a few cells, we conclude that Mad1p has a novel nuclear localization pattern.

Since some coiled–coil proteins form large insoluble oligomeric structures (Fuchs, 1994) we tested the solubility of Mad1p. Yeast extracts were made by preparing spheroplasts, douncing them and then extracting the homogenate with buffers containing various salts, detergents and nucleases. The extracts were then spun at 100,000 *g* to separate soluble from insoluble material. Pellet and supernatant fractions were then run on SDS gels and blotted for Mad1p (Fig. 6). Under all conditions the bulk of Mad1p was found in the supernatant, but we reproducibly found that a minor fraction pelleted. However, even this fraction could be solubilized by a combined treatment with 1% Triton/1 M NaCl/DNase and RNase, suggesting that Mad1p is unlikely to be a constituent of the nuclear scaffold (Mirzayan et al., 1992).

Another striking characteristic of coiled–coil proteins is

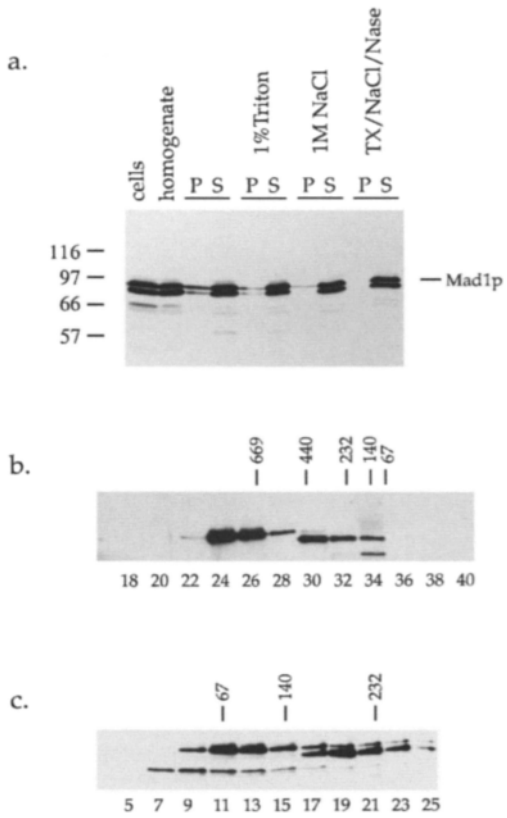

Figure 6. Mad1p solubility, sizing and sedimentation analyses. (*a*) The bulk of Mad1p behaves as a soluble protein. Yeast cells (KH 34) were spheroplasted and homogenized. Aliquots of this homogenate were then extracted with either 1% Triton X-100, 1 M NaCl or a combination of 1% Triton, 1 M NaCl, 0.25 mg/ml DNase and RNase, before being spun at 100,000 *g* for 30 min. Pellet and supernatant fractions were immunoblotted with affinity-purified anti–Mad1p antibodies. Yeast extracts were made from wild-type (KH 34) cells by bead-beating, spun at 100,000 *g* for 30 min, and then (*b*) loaded over a Superose 6 gel filtration column, or (*c*) fractionated by centrifugation through a 5–40% sucrose gradient. Fractions were immunoblotted with affinity-purified anti–Mad1p antibodies. Mad1p is the uppermost band in *b* and *c* and the molecular masses of marker proteins are indicated.

their rod shape. To assess the hydrodynamic behavior of Mad1p we fractionated yeast extracts by gel filtration and sucrose gradient sedimentation. Fig. 6 *b* shows that Mad1p behaves as a very large protein on gel filtration, running ahead of the 670-kD thyroglobulin marker. A similar size for Mad1p was obtained by immunoblotting yeast extracts that had been separated in their native state by gradient gel electrophoresis (not shown). However, Mad1p sediments relatively slowly through sucrose gradients, peaking in the same fraction as the 4.4 S BSA marker (Fig. 6 *c*). Neither the sedimentation nor the gel filtration behavior of Mad1p was altered by the presence of 1 M NaCl (not shown). Similar fractionation behavior has been reported

Figure 5. Immunofluorescent staining of yeast cells with anti-Mad1p. Wild-type (*a* and *b*) (KH 34) and *mad1Δ.1* (*c* and *d*) (KH 123] cells were stained with affinity-purified anti–Mad1p antibodies (*b* and *d*) and DAPI (*a* and *c*). Patchy nuclear staining is observed in wild-type cells and is absent in the *mad1Δ.1* cells. Wild-type diploid cells (KH 36) were stained with DAPI (*e* and *h*), anti-Mad1p (*f* and *i*), and either anti-tubulin (*g*) or pooled mAbs to the 90-kD component of the SPB (*j*). Bars, 10 μm.

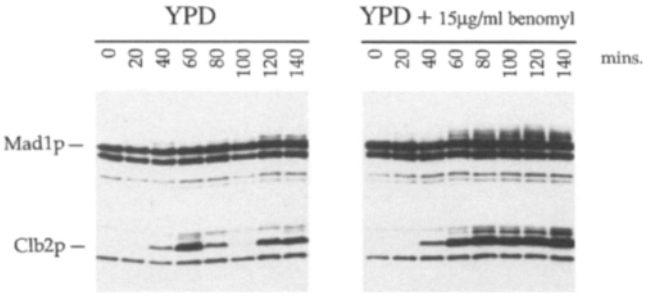

Figure 7. The ability to modify Mad1p is restricted to certain portions of the cell cycle. Wild-type (KH 34) cells were arrested with α-factor and then released into YPD or YPD containing 15 μg/ml benomyl. Cells were taken at the times indicated and extracts were immunoblotted using anti-Mad1p and anti-Clb2p antibodies.

for other coiled–coil proteins, such as myosin and kinesin (Hackney et al., 1992; Hirano and Mitchison, 1994). We therefore propose that Mad1p has a large Stokes' radius and that it may be rod shaped, consistent with the elongated structure of many coiled–coil proteins.

Modification of Mad1p by Phosphorylation

Does cell cycle progression or activation of the spindle assembly checkpoint alter the abundance or posttranslational modification of Mad1p? To answer these questions we examined cells released from a G1 arrest into normal or benomyl containing medium. Wild-type cells were arrested in G1 with α-factor and then released into YPD or YPD containing 15 μg/ml benomyl. Samples were collected over two cell cycles and analyzed for the abundance of Mad1p by immunoblotting. To monitor the timing of the cell cycle, these blots were also probed with antibodies to the mitotic cyclin Clb2p which is degraded at the end of mitosis. Fig. 7 shows that the abundance of Mad1p remains constant through the cell cycle and is not affected by benomyl-induced mitotic arrest. During a normal cell cycle there is only a minor variation in the gel mobility of Mad1p, however a significant fraction of the protein decreases in gel mobility when cells are arrested in mitosis by benomyl treatment (similar results were obtained with nocodazole; data not shown). The low level of Mad1p modification seen in untreated cells may be induced by transient spindle defects that occur in the course of normal spindle assembly. Figs. 9 and 10 clearly demonstrate that the slower migrating bands are forms of Mad1p and not cross-reacting proteins that accumulate in mitosis.

The slower migrating form of Mad1p appears in mitotically arrested cells whose levels of Clb2p are high, suggesting that modification of Mad1p is a specific response to a disrupted spindle. To test this hypothesis we asked whether Mad1p was modified when cells arrested at Start with α-factor were treated with benomyl (Fig. 8 *a*). Half of the α-factor–arrested cells were treated with 30 μg/ml benomyl in the continuous presence of α-factor to prevent their passage through Start. The other half were released from their α-factor arrest into YPD containing benomyl. Fig. 8 *a* shows that benomyl treatment of cells maintained at the α-factor arrest point causes much less modification of Mad1p than releasing cells from α-factor arrest into benomyl. The low level of Mad1p modification seen after 2 h of combined treatment with α-factor and benomyl probably represents a fraction of the cells that have broken through the α-factor arrest. This experiment shows that the modification of Mad1p is not simply a response to benomyl, but is seen only in cells in the portion of the cell cycle where spindle assembly can occur.

To determine whether other mitotic arrests are accompanied by Mad1p modification, we analyzed Mad1p in number of other mutants. Fig. 8 *b* shows that the modification of Mad1p is not seen in either *cdc23* mutants which prevent the ubiquitin-mediated proteolysis necessary to initiate anaphase and thus arrest early in mitosis with short spindles (Irniger et al., 1995), or in *cdc15* mutants which arrest later in mitosis with long spindles (Surana et al., 1993). This result demonstrates that Mad1p modification

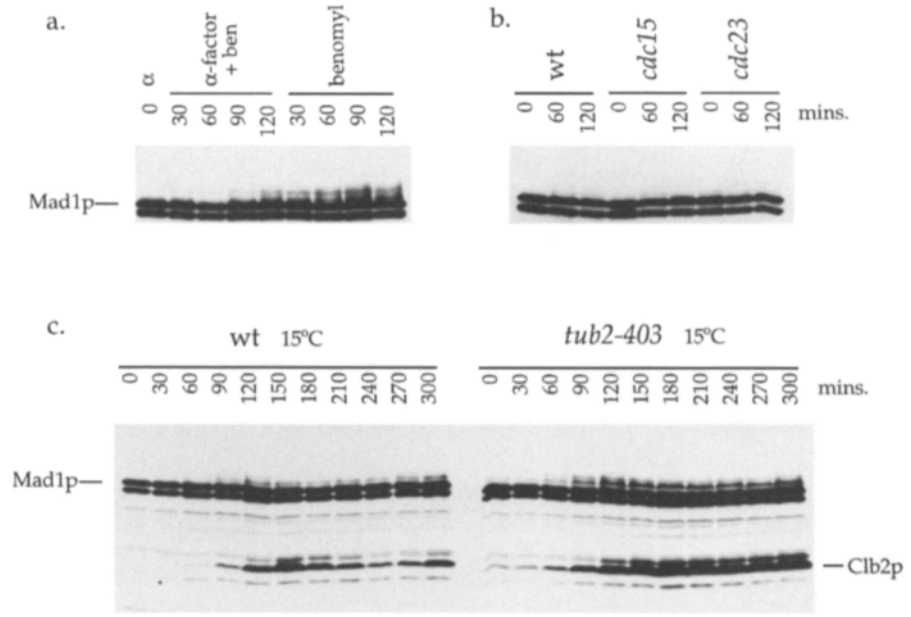

Figure 8. Mad1p is not modified when alpha-factor arrested cells are treated with benomyl, or in *cdc23* and *cdc15* mitotic arrests, but it is in a *tub2* mitotic arrest. (*a*) Wild-type cells (KH 34) were arrested with α-factor and then treated with 30 μg/ml benomyl, either with or without releasing them from the α-factor arrest. The modification of Mad1p was analyzed by immunoblotting. (*b*) Wild-type (KH 34), *cdc15-2* (KH 161), and *cdc23* (KH 162) mutants were arrested in G1 with α-factor, released, and then grown at 37°C for 2 h. The modification of Mad1p was analyzed by immunoblotting. (*c*) Wild-type (KH 146) and *tub2-403* (KH 152) cells were arrested in G1 with α-factor, released, and then grown at 15°C. Levels and modification of Clb2p and Mad1p were analyzed by immunoblotting.

requires spindle perturbations in addition to an arrest with high levels of Cdc28-Clb–associated kinase activity.

To test whether other methods of disrupting spindle microtubules lead to the modification of Mad1p, we compared synchronous cultures of wild-type and cold-sensitive *tub2-403* strains (Huffaker et al., 1988) that had been arrested with α-factor and then released at 15°C. Fig. 8 *c* shows that the *tub2* mutant arrests in mitosis with high levels of Clb2p and that a significant fraction of Mad1p is modified. In addition, we note that Mad1p is transiently modified in the wild-type cells, and that this occurs before the levels of Clb2p peak, when the spindle is presumably being assembled. Such modification can be seen in wild-type cells growing at higher temperatures (see Fig. 7) but is less obvious, consistent with it being a response to temperature-induced spindle perturbations (Dustin, 1984).

Is the reduced gel mobility of Mad1p due to phosphorylation? To test this possibility we immunoprecipitated Mad1p from logarithmically growing and benomyl-arrested cells and treated the immunoprecipitates with lambda protein phosphatase. Fig. 9 *a* shows that phosphatase treatment eliminates the slower migrating forms of Mad1p, consistent with the reduced mobility resulting from phosphorylation. Treatment with lambda protein phosphatase in the presence of phosphatase inhibitors has no effect on the gel mobility of Mad1p. As not all protein phosphorylations are accompanied by a gel shift we also analyzed Mad1p in cells that were metabolically labeled with [^{32}P]orthophosphate. Extracts were prepared from exponentially growing or cell cycle–arrested cultures, immunoprecipitated with the polyclonal anti–Mad1p antiserum, and analyzed by gel electrophoresis and autoradiography. Fig. 9 *b* shows that phosphate incorporation into Mad1p occurs to equal extents in exponentially growing, benomyl-arrested, and α-factor–arrested cells, suggesting that Mad1p is phosphorylated throughout the cell cycle. Our inability to see more slowly migrating phosphate labeled forms of Mad1p in benomyl-treated cells may reflect the relatively low level of labeling, or the poor mitotic arrest produced by benomyl treatment in low phosphate medium, or both.

We also examined the phosphorylation of the N-terminal half of Mad1p that is expressed in the *mad1Δ.1* strain. Although ^{32}P is incorporated into this fragment as efficiently as it is into the wild-type protein (Fig. 9), none of the original *mad1* alleles nor this truncated protein (not shown) show the mobility shift that occurs when wild type cells are treated with benomyl (Fig. 10 *a*). These findings indicate that Mad1p is the target for two types of phosphorylation: constitutive phosphorylation that appears to occur throughout the cell cycle and on both functional and

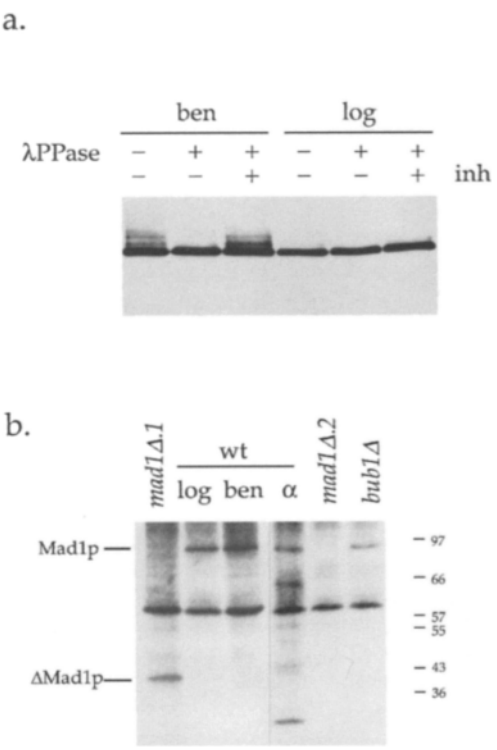

Figure 9. Mad1p is phosphorylated. (*a*) Mad1p was immunoprecipitated from wild-type extracts made from cells (KH 34) growing in YPD (*log*) or YPD with 30 μg/ml benomyl. The indicated immunoprecipitates were treated with lambda protein phosphatase, in the presence or absence of phosphatase inhibitors (*inh*), and then immunoblotted with anti-Mad1p. (*b*) Mad1p was immunoprecipitated from [^{32}P]orthophosphate-labeled cells. Wild-type cells (KH 34) were grown in low phosphate YPD medium or the same medium containing either 10 μg/ml α-factor or 30 μg/ml benomyl. The *mad1Δ.1* (KH 123), *mad1Δ.2* (KH 131), and *bub1Δ* (KH 127) cells were all grown in low phosphate YPD medium.

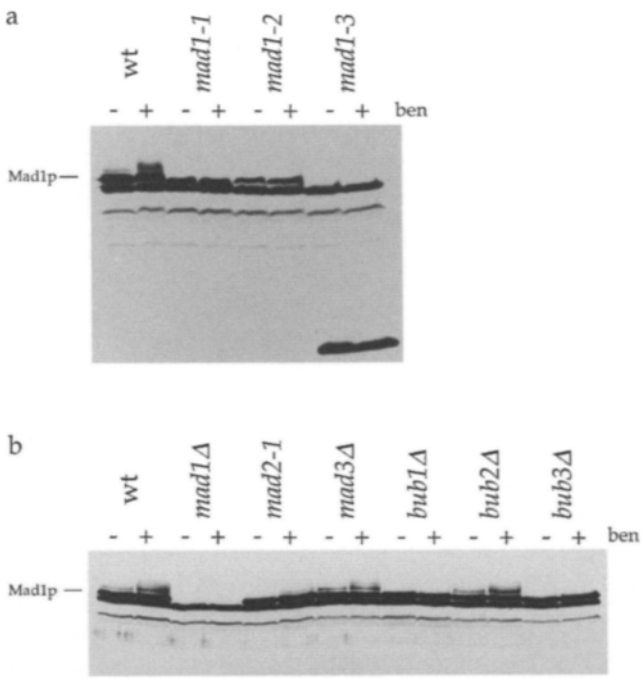

Figure 10. Hyperphosphorylation of Mad1p in spindle assembly checkpoint mutants. (*a*) Wild-type (KH 34) and the three original *mad1* alleles (BEN 24, 27, and 76) were grown to log phase and treated with 30 μg/ml benomyl for 3 h. Whole cell extracts were immunoblotted with anti-Mad1p. (*b*) Wild-type (KH 34), *mad1Δ.1* (KH 123), *mad2-1* (KH 132), *mad3Δ* (KH 125), *bub1Δ* (KH 127), *bub2Δ* (KH 128), and *bub3Δ* (MAY 2072) strains were grown to log phase, and then treated with 30 μg/ml benomyl for 3 h. Whole cell extracts were made and immunoblotted with anti-Mad1p.

non-functional forms of Mad1p, and a regulated phosphorylation that is induced by activation of the spindle assembly checkpoint and occurs only on functional Mad1p.

We asked whether Mad1p was hyperphosphorylated in mutants defective in the spindle assembly checkpoint. To do this we examined the gel mobility of Mad1p in extracts made from wild type, *mad*, or *bub* strains that were grown in the absence or presence of 30 μg/ml benomyl. Fig. 10 *b* shows that Mad1p hyper-phosphorylation was undiminished in the *mad3Δ* and *bub2Δ* mutants, from which we conclude that neither Mad3p nor Bub2p are necessary for this modification of Mad1p. However, the hyperphosphorylation of Mad1p was dramatically reduced in *mad2-1*, and absent in the *bub1Δ* and *bub3Δ* mutant strains. This shows that Bub1p, Bub3p, and Mad2p are all important for this modification of Mad1p. The observation that Bub1p is a novel protein kinase (Roberts et al., 1994) prompted us to ask whether this protein is required for all phosphorylation events on Mad1p. Mad1p is still phosphate labeled in the *bub1Δ* strain showing that Bub1p is not required for the addition of all phosphate groups to Mad1p (Fig. 9 *b*).

Discussion

We have cloned the *MAD1* gene and shown that it encodes a novel nuclear phosphoprotein that is predicted to form coiled–coils. Like the previously isolated *mad1* alleles, *mad1Δ* cells are unable to delay initiation of anaphase in response to microtubule depolymerization and thus suffer a high frequency of chromosome loss and rapid death upon treatment with anti-microtubule drugs. Spindle disruption is accompanied by a Mad1p phosphorylation that reduces the mobility of the protein and this modification requires the Bub1p, Bub3p and Mad2p functions, but not Bub2p and Mad3p, suggesting that this phosphorylation plays an important role in the spindle assembly checkpoint.

Antibodies to Mad1p reveal that the protein has a non-uniform distribution within the nucleus. All cells show a diffuse punctate staining and many also have a small number of brightly staining foci. Neither staining pattern reproducibly colocalizes with nuclear pores, spindle–pole bodies or telomeres, suggesting that the Mad1p may be found at a novel location within the nucleus. Identifying the Mad1p-containing structures will require immunoelectron microscopy or isolating Mad1p homologs from organisms with better cytology. In cell extracts Mad1p is largely soluble, and its hydrodynamic behavior suggests that Mad1p has an elongated shape like many other coiled-coil proteins.

Analyzing the gel mobility and phosphate labeling of Mad1p has revealed both a constitutive level of phosphorylation, seen in all stages of the cell cycle that we analyzed, and a hyper-phosphorylation induced by spindle depolymerization. The former phosphorylation is seen in exponentially growing cells as well as in G1 and mitotically arrested cells, suggesting that it occurs throughout the cell cycle. We do not know the identity of the constitutive phosphorylation site(s), or whether their modification plays any role in the spindle assembly checkpoint. The regulated phosphorylation reduces the gel mobility of Mad1p and is seen only in those parts of the cell cycle in which cells are able to assemble a spindle. The modification is detectable at a low level in normally growing cells, and is much more pronounced in benomyl treated cells suggesting that it may be induced by activation of the spindle assembly checkpoint. The low level of Mad1p hyperphosphorylation in wild type cells could either reflect full activation of the spindle assembly checkpoint in a small fraction of the population with transient spindle defects, or weak activation in all cells during the course of spindle assembly. We find that wild-type cells growing in the cold show higher levels of Mad1p modification, and that the *tub2-403* mutant arrests in the cold in mitosis with hyperphosphorylated Mad1p, showing that Mad1p modification is not solely a response to drug-induced spindle perturbations. In addition we find that Mad1p receives little modification in *cdc23* and *cdc15* mutant arrests, ruling out the possibility that the hyperphosphorylation of Mad1p is simply a by-product of any cell cycle arrest with active Cdc28–Clb2 complexes. But if *cdc23* mutants are first arrested at 37°C and then treated with benomyl without releasing them from the arrest Mad1p does become hyperphosphorylated (data not shown), showing that spindle disassembly at this metaphase-like arrest can be readily detected by the checkpoint.

Examining Mad1p hyper-phosphorylation in *mad* and *bub* mutants strengthens the case that this modification plays an important role in the spindle assembly checkpoint. There is no mobility shift in *mad1-1*, *mad1-2*, *mad1-3*, or *mad1Δ.1*. This observation suggests that the proper function of Mad1p is needed for its own modification and is especially significant for *mad1-2*, which encodes an apparently full length protein. The modification of wild-type Mad1p does not occur in the *bub1* and *bub3* mutants and is strongly reduced in the *mad2* mutant. Although the correlative evidence is strong, proof that Mad1p hyperphosphorylation is necessary for the spindle assembly checkpoint will require the identification and mutation of the regulated Mad1p phosphorylation sites.

We assume that the spindle assembly checkpoint must consist of at least three classes of component: a detection system that monitors the structure of the spindle, a signal transduction pathway that relays this information, and a target in the cell cycle machinery whose regulation can produce a mitotic arrest. Even if the mobility shift of Mad1p is no more than a correlation with the activation of the spindle assembly checkpoint, it represents the first tool for ordering the functions in this pathway. The simplest interpretation of our data is that Mad1p lies in the middle of the checkpoint pathway and that mutants that fail to hyperphosphorylate this protein identify proteins that act upstream of Mad1p, whereas mutants that can modify Mad1p identify proteins that act downstream of Mad1p (Fig. 11). Clearly our results do not allow us to rule out other more complicated models. For example, Bub2p and Mad3p need not be directly downstream of Mad1p but could instead be in a parallel pathway whose action is required for cell cycle arrest but not for the hyperphosphorylation of Mad1p. The isolation of dominant alleles of *MAD1*, and of the other *MAD* and *BUB* genes, that cause a mitotic arrest should enable us to order the function of these genes within the spindle assembly checkpoint more precisely.

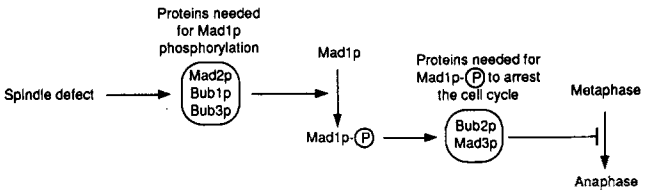

Figure 11. A model suggesting the order of function in the spindle assembly checkpoint. See text for details.

Previous work identifies three candidates for the physiological Mad1p kinase. The demonstration that Bub1p is a protein kinase that can phosphorylate itself and Bub3p in vitro (Roberts et al., 1994), and the inability of *bub1* cells to hyperphosphorylate Mad1p make Bub1p a good candidate for a Mad1p-kinase. The *MPS1* gene product is another candidate, since it has protein kinase activity in vitro and is required for the spindle assembly checkpoint to detect defects in spindle pole body duplication (Weiss, E., and M. Winey, personal communication). Finally, the observation that activation of the spindle assembly checkpoint in frog egg extracts requires the activities of MAP kinases suggests that members of this kinase family are also candidates for the Mad1p kinase (Minshull et al., 1994). By identifying the sites of benomyl-dependent Mad1p phosphorylation we hope to determine their role in the spindle assembly checkpoint and to identify the kinases and phosphatases that regulate this modification.

We would like to thank Tibor Roberts, Andy Hoyt, Rong Li, Jeremy Minshull, Tim Stearns, Eric Weiss, and Mark Winey for yeast strains and plasmids; Doug Kellogg, John Kilmartin, and David Shore for antibodies; Cathy Mistrot for her expert technical assistance; and Rey Huei Chen, Sandra Holloway, Lena Hwang, Doug Kellogg, Jeremy Minshull, Alison Pidoux, Adam Rudner, Dana Smith, Aaron Straight, and Bill Wells for valuable discussions and their critical reading of the manuscript.

K. G. Hardwick is supported by a Visiting U.K. Fellowship from the Lucille P. Markey Charitable Trust. A. W. Murray is a David and Lucile Packard fellow. This work was supported by grants from the National Institute of Health, the Markey Charitable Trust, the Packard Foundation, and the March of Dimes.

Received for publication 30 August 1994 and in revised form 2 August 1995.

References

Adams, A. E. M., and J. R. Pringle. 1984. Relationship of actin and tubulin distribution in wild-type and morphogenetic mutant *Saccharomyces cerevisiae*. *J. Cell Biol.* 98:934–945.

Al-Khodairy, F., and A. M. Carr. 1992. DNA repair mutants defining G2 checkpoint pathwys in *S. pombe*. *EMBO J.* 11:1343–1350.

Al-Khodairy, F., E. Fotou, K. S. Sheldrick, D. J. Griffiths, A. R. Lehmann, and A. M. Carr. 1994. Identification and characterization of new elements involved in checkpoint and feedback controls in fission yeast. *Mol. Biol. Cell.* 5:147–160.

Al-Khodairy, F., T. Enoch, I. M. Hagan, and A. M. Carr. 1995. The *S. pombe hus5* gene encodes a ubiqutin conjugatin enzyme required for normal mitosis. *J. Cell Sci.* 108:475–486.

Callan, H. G., and P. A. Jacobs. 1957. The meiotic process in *Mantis religiosa* L. males. *J. Genet.* 55:200–217.

Dingwall, C., and R. A. Laskey. 1991. Nuclear targeting sequences—a consensus? *Trends Biochem. Soc.* 16:478–481.

Dustin, P. 1984. Microtubules. Springer-Verlag, New York.

Enoch, T., A. M. Carr, and P. Nurse. 1992. Fission yeast genes involved in coupling mitosis to DNA replication. *Genes & Dev.* 6:2035–2046.

Enoch, T., and P. Nurse. 1990. Mutation of fission yeast cell cycle control genes abolishes dependence of mitosis on DNA replication. *Cell.* 60:665–673.

Ford, J. C., F. Al-Khodairy, E. Fotou, K. S. Sheldrick, D. J. Griffiths, and A. M. Carr. 1994. 14-3-3 protein homologs required for the DNA damage checkpoint in fission yeast. *Science (Wash. DC).* 265:533–535.

Fuchs, E., and K. Weber. 1994. Intermediate filaments: structure, dynamics and disease. *Annu. Rev. Biochem.* 63:345–382.

Futcher, B., and J. Carbon. 1986. Toxic effects of excess cloned centromeres. *Mol. Cell Biol.* 6:2213–2222.

Hackney, D. D., J. D. Levitt, and J. Suhan. 1992. Kinesin undergoes a 9S to 6S conformational transition. *J. Biol. Chem.* 267:8696–8701.

Harlow, E., and D. Lane. 1988. Antibodies: A Laboratory Manual. Cold Spring Harbor Laboratory, Cold Spring Harbor, NY.

Hartwell, L. H., and T. A. Weinert. 1989. Checkpoints: controls that ensure the order of cell cycle events. *Science (Wash. DC).* 246:629–634.

Henikoff, S. 1984. Unidirectional digestion with exonuclease III creates targeted breakpoints for DNA sequencing. *Gene.* 28:351–359.

Hirano, T., and T. J. Mitchison. 1994. A heterodimeric coiled-coil protein required for mitotic chromosome condensation in vitro. *Cell.* 79:449–458.

Holloway, S. L., M. Glotzer, R. W. King, and A. W. Murray. 1993. Anaphase is initiated by proteolysis rather than by the inactivation of MPF. *Cell.* 73: 1393–1402.

Hoyt, M. A., L. Trotis, and B. T. Roberts. 1991. *S. cerevisiae* genes required for cell cycle arrest in response to loss of microtubule function. *Cell.* 66:507–517.

Huffaker, T. C., J. H. Thomas, and D. Botstein. 1988. Diverse effects of β-tubulin mutations on microtubule formation and function. *J. Cell Biol.* 106:1997–2010.

Hussain, M., and J. Lenard. 1991. Characterization of *PDR4*, a *Saccharomyces cerevisiae* gene that confers pleiotropic drug resistance in high-copy number. *Gene.* 101:149–152.

Irniger, S., S. Piatti, C. Michaelis, and K. Nasmyth. 1995. Genes involved in sister chromatid separation are needed for B-type cyclin proteolysis in budding yeast. *Cell.* 77:1037–1050.

Klein, F., T. Laroche, M. E. Cardenas, J. F. Hofman, D. Schweizer, and S. M. Gasser. 1992. Localization of RAP1 and topoisomerase II in nuclei and meiotic chromosomes of yeast. *J. Cell Biol.* 117:935–948.

Li, R., and A. W. Murray. 1991. Feedback control of mitosis in budding yeast. *Cell.* 66:519–531.

Li, X., and R. B. Nicklas. 1995. Mitotic forces control a cell cycle checkpoint. *Nature (Lond.).* 373:630–632.

Lupas, A., M. Van Dyke, and J. Stock. 1991. Predicting coiled coils from protein sequences. *Science (Wash. DC).* 252:1162–1164.

Minshull, J., H. Sun, N. K. Tonks, and A. W. Murray. 1994. MAP-kinase dependent mitotic feedback arrest in *Xenopus* egg extracts. *Cell.* 79:475–486.

Mirzayan, C., C. S. Copeland, and M. Snyder. 1992. The NUF1 gene encodes an essential coiled-coil related protein that is a potential component of the yeast nucleoskeleton. *J. Cell Biol.* 116:1319–1332.

Morgan, D. O. 1995. Principles of CDK regulation. *Nature (Lond.).* 374:131–134.

Moye-Rowley, W. S., K. D. Harshman, and C. S. Parker. 1989. Yeast *YAP1* encodes a novel form of the jun family of transcriptional activator proteins. *Genes & Dev.* 3:283–292.

Murray, A. W. 1994. Cell cycle checkpoints. *Curr. Opin. Cell Biol.* 6:872–876.

Murray, A. W. 1995. The genetics of cell cycle checkpoints. *Curr. Opin. Genet.* 5:5–11.

Nakajima, H., A. Hirata, Y. Ogawa, T. Yonehara, K. Yoda, and M. Yamasaki. 1991. A cytoskeleton-related gene, *USO1*, is required for intracellular protein transport in *Saccharomyces cerevisiae*. *J. Cell Biol.* 113:245–260.

Norbury, C., and P. Nurse. 1992. Animal Cell Cycles and Their Control. *Annu. Rev. Biochem.* 61:441–470.

Philippsen, P., A. Stotz, and C. Scherf. 1991. DNA of *Saccharomyces cerevisiae*. *Methods Enzymol.* 194:169–181.

Rieder, C. L., A. Schultz, R. Cole, and G. Sluder. 1994. Anaphase onset in vertebrate somatic cells is controlled by a checkpoint that monitors sister kinetochore attachment to the spindle. *J. Cell Biol.* 127:1301–1310.

Roberts, R. T., K. A. Farr, and M. A. Hoyt. 1994. The *Saccharomyces cerevisiae* checkpoint gene *BUB1* encodes a novel protein kinase. *Mol. Cell. Biol.* 14: 8282–8291.

Rose, M. D., P. Novick, J. H. Thomas, D. Botstein, and G. R. Fink. 1987. A *Saccharomyces cerevisiae* genomic plasmid bank based on a centromere-containing shuttle vector. *Gene.* 60:237–243.

Rout, M. P., and J. V. Kilmartin. 1990. Components of the yeast spindle and spindle pole body. *J. Cell Biol.* 111:1913–1927.

Rowley, R., S. Subramani, and P. G. Young. 1992. Checkpoint controls in *Schizosacchoramyces pombe: rad1*. *EMBO J.* 11:1335–1342.

Rubin, G. M. 1975. Preparation of RNA and ribosomes from yeast. *Methods Cell Biol.* XII:45–64.

Schnell, N., B. Krems, and K. D. Entian. 1992. The PAR1 (YAP1/SNQ3) gene of Saccharomyces cerevisiae, a c-jun homologue, is involved in oxygen metabolism. *Curr. Genet.* 21:269–273.

Sherman, F., G. Fink, and C. Lawrence. 1974. Methods in Yeast Genetics. Cold Spring Harbor Laboratory Press, Cold Spring Harbor, NY.

Sikorski, R. S., and P. Hieter. 1989. A system of shuttle vectors and yeast host strains designed for efficient manipulation of DNA in *Saccharomyces cerevisiae*. *Genetics.* 122:19–27.

Smith, D. B., and K. S. Johnson. 1988. Single-step purification of polypeptides expressed in *Escherichia coli* as fusions with glutathione S-transferase. *Gene.* 67:31–40.

Spencer, F., and P. Hieter. 1992. Centromere DNA mutations induce a mitotic

delay in *Saccharomyces cerevisiae. Proc. Natl. Acad. Sci. USA.* 89:8908–8912.
Stearns, T., M. Hoyt, A., and D. Botstein. 1990. Yeast mutants sensitive to antimicrotubule drugs define three genes that affect microtubule function. *Genetics.* 124:251–262.
Surana, U., A. Amon, C. Dowzer, J. McGrew, B. Byers, and K. Nasmyth. 1993. Destruction of the CDC28/CLB mitotic kinase is not required for the metaphase to anaphase transition in budding yeast. *EMBO J.* 12:1969–1978.
Ward, G. E., and M. W. Kirschner. 1990. Identification of cell cycle-regulated phosphorylation sites on nuclear lamin C. *Cell.* 61:561–577.
Weinert, T. A., and L. H. Hartwell. 1988. The RAD9 gene controls the cell cycle response to DNA damage in Saccharomyces cerevisiae. *Science (Wash. DC).* 241:317–322.
Weinert, T. A., G. L. Kiser, and L. H. Hartwell. 1994. Mitotic checkpoint genes in budding yeast and the dependence of mitosis on DNA replication and repair. *Genes & Dev.* 8:652–665.
Wu, A., J. A. Wemmie, N. P. Edgington, M. Goebl, J. L. Guevara, and W. S. Moye-Rowley. 1993. Yeast bZip proteins mediate pleiotropic drug and metal resistance. *J. Biol Chem.* 268:18850–18858.
Yang, C. H., E. J. Lambie, and M. Snyder. 1992. NuMA: an unusually long coiled-coil related protein in the mammalian nucleus. *J. Cell Biol.* 116:1303–1317.
Yen, T. J., G. Li, B. T. Schaar, I. Szilak, and D. W. Cleveland. 1992. CENP-E is a putative kinetochore motor that accumulates just before mitosis. *Nature (Lond.).* 359:536–539.